Journal of Power Sources 194 (2009) 683–689

Contents lists available at ScienceDirect

Journal of Power Sources

journal homepage: www.elsevier.com/locate/jpowsour

High catalytic performance and stability of Pt/C using acetic acid functionalized carbon

Jilei Ye [a], Jianguo Liu [a,b,*], Yi Zhou [a], Zhigang Zou [a,b,**], Jun Gu [a], Tao Yu [a]

[a] Eco-materials and Renewable Energy Research Center, Department of Physics and National Laboratory of Solid State Microstructures, Nanjing University, Nanjing 210093, People's Republic of China
[b] Department of Materials Science and Engineering, Nanjing University, Nanjing 210093, People's Republic of China

ARTICLE INFO

Article history:
Received 10 April 2009
Received in revised form 10 June 2009
Accepted 10 June 2009
Available online 18 June 2009

Keywords:
Fuel cell
Platinum supported on carbon
Carbon modification
Acetic acid treatment

ABSTRACT

Carbon (Vulcan XC-72, Cobat Corp.) is pretreated using acetic acid (HAC) before the Pt deposition by microwave assisted glycol method. TEM and XRD results indicate that 3 nm Pt nano-particles are uniformly dispersed on the surface of modified XC-72. In order to examine the interaction between Pt nano-particles and carbon, Pt/C-HAC and commercial Pt/C (Johnson Matthey Corp.) are calcined at 500 °C for 2 h under nitrogen atmosphere. The average Pt particle size of Pt/C-HAC after calcination is only 10–12 nm in diameter while commercial Pt particles grow up to 25–35 nm with a broad size distribution. Meanwhile, electrochemical studies of Pt/C-HAC reveal higher activity and stability for both methanol oxidation and oxygen reduction than that of Pt/C-JM. The pore structure and surface composition are investigated by BET and XPS, which implies that much microporous structure and carbonyl functional groups on carbon surface are obtained after HAC treatment. The high catalytic performance and stability might mainly be due to the strong interaction between Pt nano-particles and carbon by carbonyl functional groups. Therefore, HAC treatment is proved to be a facile and effective method for carbon as the support for Pt as fuel cell catalyst.

1. Introduction

Carbon has played critical function as supports of Pt in proton exchange membrane fuel cells because the activity, selectivity and stability of electrocatalysts are greatly influenced by surface microstructure and chemical property of carbon [1–4]. But as-received carbon materials without treatment have lots of disadvantages, such as much ash content and hydrophobic surface, which will result in poor ability to support Pt. Therefore, surface modification of carbon, which can enhance the attachment and anchoring of nano-sized Pt particles, has attracted much attention in recent years [5–8]. Chemical modifications by HNO_3, H_2SO_4 or H_2O_2 at moderate temperature are usually used to improve surface polarity and oxygen-containing groups [9–15]. The participation of functional groups such as hydroxyl, carboxyl and carbonyl on carbon surfaces improves platinum dispersion and thereby obtain high electrochemical activity [16,17]. However, oxidation treatment with strong acids or oxidation also gives rise to the destruction microporous structure, thus the surface area and adsorption capability of carbon decrease [18]. Furthermore, these strong acids or oxidations often require many steps to remove before Pt nano-particle deposition [19–21]. Recently, citric acid, as a weak acid, was reported to functionalize carbon as catalyst support, which improved the activity of methanol electro-oxidation [22]. However, the microstructure of carbon support after modification and the stability, which are also very important for fuel cell in long running time, have not been reported. To analyze the different structure of carbon support modified by weak acids, we altered a simple acid, acetic acid, to functionalize the carbon support and then investigated the catalytic performance for methanol electro-oxidation.

In this study, carbon treatment at room temperature by acetic acid (HAC) was evaluated to functionalize XC-72 (Vulcan, Colbalt Company). The obvious increase of functional groups and micropores of carbon was found by XPS and BET analysis. Cyclic voltammetry (CV) results demonstrated that Pt supported on XC-72 with HAC modification has a higher electrochemical surface area, catalytic activity for methanol oxidation and oxygen reduction than that of commercial Pt/C catalyst. Especially, XRD and TEM results obviously exhibited that Pt nano-particles supported HAC modified carbon was more stable than commercial Pt/C catalyst. Pt/C-HAC catalyst showed higher stability due to the strong interaction between Pt and carbon support. It indicates that carbon

* Corresponding author at: ERERC, Department of Materials Science and Engineering, Nanjing University, 22 Hankou Road, Nanjing 210093, People's Republic of China. Tel.: +86 25 83621219.
** Corresponding author at: ERERC, Department of Physics, Nanjing University, 22 Hankou Road, Nanjing 210093, People's Republic of China. Tel.: +86 25 83686630.
E-mail addresses: jianguoliu@nju.edu.cn (J. Liu), zgzou@nju.edu.cn (Z. Zou).

0378-7753/$ – see front matter © 2009 Elsevier B.V. All rights reserved.
doi:10.1016/j.jpowsour.2009.06.032

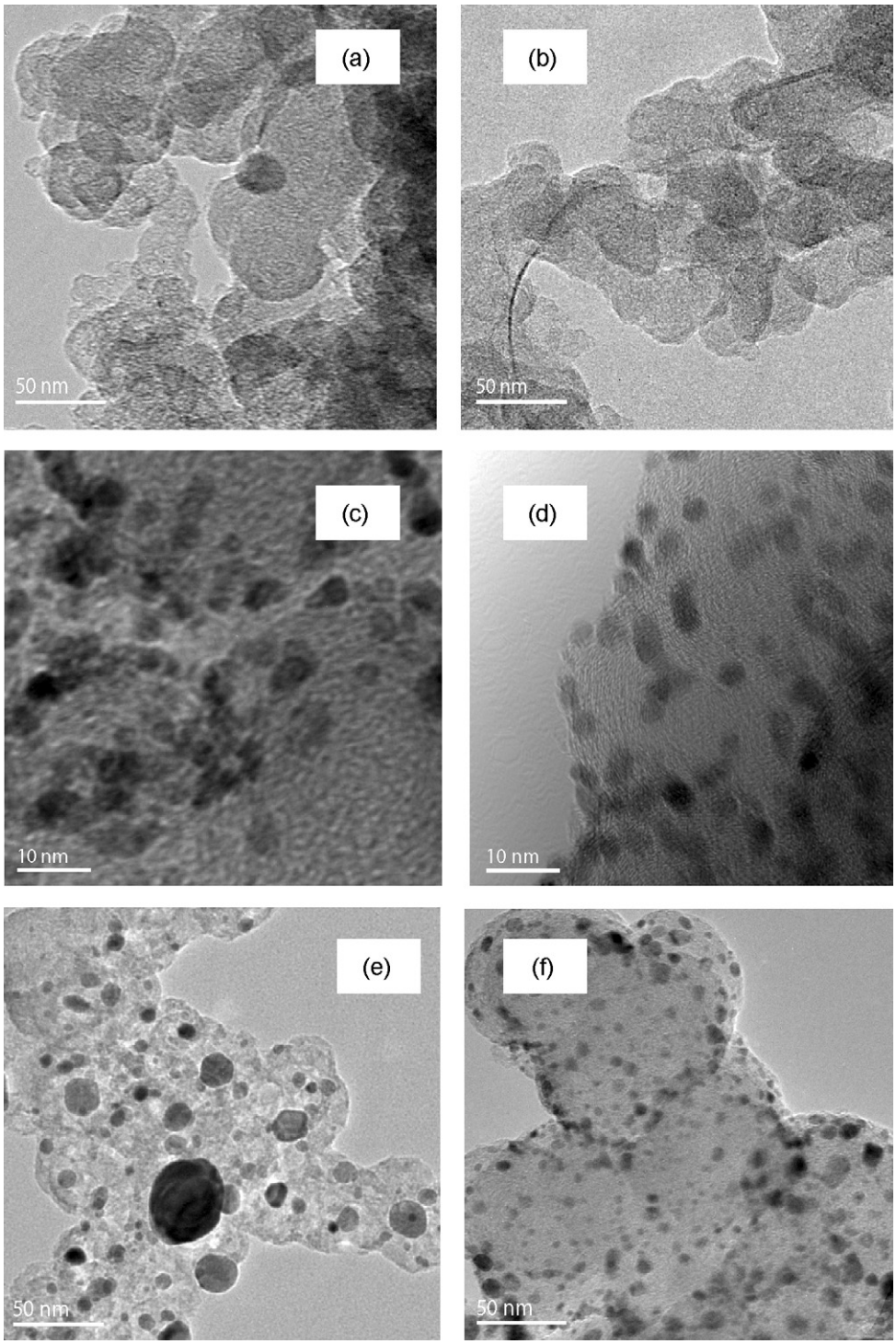

Fig. 1. TEM images of XC-72 and Pt/C before and after HAC treatment: (a) C-as received; (b) C-HAC; (c) 40% Pt/C-JM; (d) 40% Pt/C-HAC; (e) 40% Pt/C-JM-500 °C; (f) 40% Pt/C-HAC-500 °C.

support by HAC modification is a promising method to improve electrocatalyst performance for fuel cell applications.

2. Experimental

2.1. Samples preparation

XC-72 with a weight of 1 g from Cobat Corp. was mixed ultrasonically with 1 ml HAC and 100 ml deionized water, for 15 min at room temperature. Then carbon suspension was filtrated and heated at 300 °C for 30 min to remove the absorbed water. The acetic acid modification of XC-72 was marked as C-HAC.

Microwave-assisted heating method was chosen to prepare Pt/C catalysts in ethylene glycol (EG) solution with H_2PtCl_6 as precursor. Firstly, 120 mg of C-HAC was dispersed in 30 ml ethylene glycol by ultrasonic vibration, and then mixed with 10.8 ml H_2PtCl_6 glycol solution of 0.02 M. The pH value was adjusted around 9 by adding 1.0 M NaOH/ethylene glycol solution. After continuous stirring for 4 h, the beaker was placed in the center of a household microwave

Table 1
BET surface area and pore size of XC-72 samples.

Samples	BET ($m^2\ g^{-1}$)	Average pore size (nm)	Micropore volume ($cm^3\ g^{-1}$)	Total pore volume ($cm^3\ g^{-1}$)	V_{micro}/V_{total} (%)
C-as received	227.4	6.8	0.0298	0.386	7.72
C-HAC	231.2	6.0	0.0317	0.366	8.66
C-HNO_3	178.9	7.3	0.0257	0.326	7.88
40% Pt/C-JM	143.6	8.3	–	–	
40% Pt/C-HAC	177.0	8.1	–	–	

oven (2450 MHz, 700 W) and heated intermittently every 10 s in 30 s period for 10 times. 1 M hydrochloric acid was dropped in the solution as the sedimentation promoter until pH 3. Finally, the sample was filtered, washed and dried at 80 °C for 12 h in a vacuum oven. The as-prepared 40 wt% Pt/C catalysts with C-HAC are denoted as and Pt/C-HAC. 40 wt% Pt/C catalysts from Johnson Matthey Corp. were used for comparison, which was denoted as Pt/C-JM.

2.2. Physical and electrochemical characterizations

The particle-size distribution and morphology of catalysts were examined by transmission electron microscope (TEM) on a FEI Tecnai20 FEG at 200 kV. X-ray diffraction (XRD) measurements were carried out with a Rigaku D/MAX-Ultima β X-ray diffractometer using Cu Kα radiation (λ = 0.15406 nm). The 2θ angular ranges between 20° and 80° were explored at a scan rate of 5° min^{-1}. Nitrogen adsorption porosimetry was performed with Micromeritics TriStar 3000 system. Samples were outgassed at 150 °C under nitrogen flow for about 3 h prior to analysis. The specific surface area was calculated using Brunauer–Emmett–Teller (BET) equation. The X-ray photoelectron spectroscopy (XPS) measurement was performed by ESCALAB 250 apparatus, using monochromated Al Kα radiation at 150 W, in the pass energy (PE) mode (PE = 20 eV). All of the spectra were obtained under identical conditions. The pressure of the spectrometer was 5×10^{-10} mbar and 5×10^{-9} mbar during the measurements. The regional XPS of C 1s and O 1s were deconvoluted by using the multipak software to identify different carbon and oxygen species.

Electrochemical experiments were performed by PARSTAT 2273 electrochemical workstation (Princeton Applied Research) equipped with a three-electrode configuration using Pt foil as a counter electrode and saturated calomel electrode (SCE) as a reference. The work electrodes were fabricated by casting Nafion-impregated catalyst ink onto glass carbon electrode with an area of 0.196 cm^2. The loading of the catalyst was 0.255 mg cm^{-2}. For CV measurements, the catalyst as working electrode was immersed in nitrogen saturated 0.5 M H_2SO_4 with or without 0.5 M CH_3OH solution. For oxygen reduction reaction (ORR), oxygen gas was bubbled into 0.5 M H_2SO_4 for 30 min.

3. Results and discussion

3.1. TEM analysis and XRD characterization

Fig. 1 shows TEM images of carbons, commercial and as-prepared Pt/C catalysts before and after calcination. As shown in Fig. 1a and b, particle size of XC-72 after the HAC treatment decreased slightly compared with as-received one. Most importantly, carbon after HAC treatment demonstrated a narrower distribution, which is favorable to support Pt nano-particles. For 40 wt% Pt/C-JM in Fig. 1c, Pt nano-particles present on the carbon support with a size distribution between 3 nm and 5 nm. As illustrated from Fig. 1d, the mean size of Pt particles was concentrated around 3.0 nm and highly dispersed on C-HAC, which is significantly important for increasing catalyst activity. As reported by literature [18], the strong oxidation of carbon by HNO_3, H_2SO_4 or H_2O_2 treatment will result in the collapse of microspores and decrease its supporting capacity. Here, the results indicate that acetic acid modification of carbon will not destroy the structure of carbon and effectively enhances homogeneous dispersion of Pt.

It was reported that Pt nano-particles tend to congregate and get bigger after long-term operation in fuel cell [23,24]. The growth of Pt particle leads to the decrease of electrochemistry surface area, and the performance will decay seriously. In order to examine the stability, Pt/C catalysts were calcined at 500 °C under nitrogen atmosphere. As shown in Fig. 1e and f, Pt particles obviously increased after calcination for both Pt/C-JM and Pt/C-HAC. For Pt/C-JM catalyst, most of Pt particles size ranged around 15 nm, some particles grew even up to 40 nm. However, Pt/C-HAC catalyst showed a uniform distribution centered around 10 nm. No larger Pt particles than 12 nm appeared on C-HAC support. It indicated that the interaction between Pt particles and carbon was enhanced significantly after HAC treatment, which would exhibit the high potential stability during fuel cell operation.

The XRD patterns of Pt/C-JM and Pt/C-HAC are given in Fig. 2. The diffraction peaks center face cubic crystalline (fcc) Pt, namely (1 1 1), (2 0 0) and (2 2 0) at 39.6°, 46.3° and 67.4° demonstrated the presence of Pt in metallic form [25]. The average crystalline size of Pt particles for Pt/C-JM and Pt/C-HAC, as calculated by the Sherrer formula at 2θ = 67.4°, was about 3.1 nm. It was consistent with the results from TEM images in Fig. 1c. In addition, the peak intensity of Pt relative to C(0 0 2) was stronger in Pt/C-HAC catalyst than in Pt/C-JM catalysts, which may be a signal of higher density Pt particles on modified carbon support. From XRD patterns of (c) and (d), Pt particles grew much larger after calcination at 500 °C for Pt/C catalyst. However, it was worth noting that the aggregation in Pt/C-HAC catalyst was less serious than that of Pt/C-JM catalyst as the similar result of TEM results in Fig. 1e and f.

3.2. BET characterization

The BET and pore size of carbon by different methods of treatment are shown in Table 1. The BET surface area of XC-72

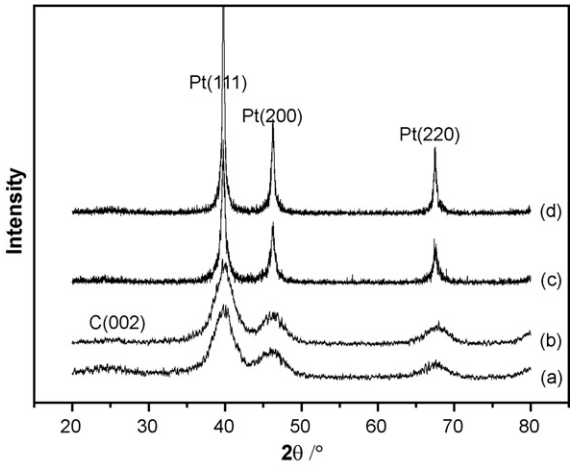

Fig. 2. XRD patterns of Pt/C catalysts: (a) Pt/C-JM; (b) Pt/C-HAC; (c) Pt/C-JM calcined at 500 °C; (d) Pt/C-HAC calcined at 500 °C.

Table 2
XPS data of all samples.

Samples	C 1s		O 1s		Pt 4f	
	Binding energy (eV)	Relative ratio (%)	Binding energy (eV)	Relative ratio (%)	Binding energy (eV)	Relative ratio (%)
C-as received	284.4 (C_α)	69.4	–	–	–	–
	285.6–286.6 (C_β)	25.0	532.2 (O_β)	55.2	–	–
	289.0 (C_γ)	5.6	533.5 (O_γ)	44.8		
C-HAC	284.4 (C_α)	58.1			–	–
	285.7–286.6 (C_β)	34.4	532.1 (O_β)	58.8	–	–
	288.9 (C_γ)	7.6	533.4 (O_γ)	41.2		
40% Pt/C-JM	284.4 (C_α)	66.2	530.6 (O_α)	11.9	71.1 ($4f_{5/2}$)	–
	285.3–286.6 (C_β)	27.8	532.0 (O_β)	49.8	74.4 ($4f_{7/2}$)	–
	288.8 (C_γ)	6.0	533.4 (O_γ)	38.3		
40% Pt/C-HAC	284.6 (C_α)	49.8	530.7 (O_α)	5.9	71.3 ($4f_{5/2}$)	–
	285.4–286.6 (C_β)	40.8	532.3 (O_β)	45.1	74.6 ($4f_{7/2}$)	–
	288.9 (C_γ)	9.5	533.6 (O_γ)	49.2		

decreased from 227.4 $m^2\,g^{-1}$ to 178.9 $m^2\,g^{-1}$ after treated by HNO_3, as reported in previous literature [18]. Simultaneously, the average pore size enlarged to 7.3 nm from 6.8 nm, which meant the surface micropore structure may be damaged and carbon particles aggregate after HNO_3 modification [26]. However, acetic acid treatment of carbon had little effect on BET surface area. According to the result of pore distribution in Table 1, the pore volume of carbon changed after HAC treatment. For as-received XC-72, there are commonly two major types of pores: 2–4 nm of micropores and 30–100 nm of accumulation pores. HAC treatment made the micropore volume of carbon increase from 0.0298 $cm^3\,g^{-1}$ to 0.0317 $cm^3\,g^{-1}$, which was in favor of supporting Pt nano-particles. Additionally, as-prepared Pt/C-HAC catalyst had a surface area of 177.0 $m^2\,g^{-1}$, while Pt/C-JM only was 143.6 $m^2\,g^{-1}$.

3.3. XPS analysis

The surface functional groups, such as carboxyl, lactone, carbonyl, and hydroxyl, are generally analyzed by FT-IR technique [22,27]. However, it is not easy to precisely quantify the surface species, which is due to the small quantity of functional groups on weakly oxidized carbon. Here, XPS technique was used to investigate the change of surface element. Fig. 3 and Table 2 show the XPS results of Pt 4f, C 1s and O 1s. The binding energy (BE) of each peak was referenced to a C 1s value of 284.6 eV.

According to Fig. 3, multi forms of oxygen atoms and carbon atoms were found in all samples. The oxygen signal around 532.2 eV and 533.3 eV were due to –C═O and —CO, respectively marked as O_β and O_γ [28]. The main C 1s spectrum at binding energy of 284.6 eV was ascribed to graphitic carbon (C—C). The peak around 285.6–286.6 eV was assigned to carbonyl species (—C═O) [29,30]. A low intensity band observed around 288.9 eV could be attributed to either —COO or carbonate. The highly oxidized carbon signal was reported by Goodenough et al. [31], but no precise identification of the species could be made so far. The three kinds of carbon species were labels as C_α, C_β, C_γ.

It can be seen from Table 2 that the ratio of oxygen atoms in surface elements increased from 7.9% of C-as received to 13.3% of C-HAC. Correspondingly, the ratio of carbon atoms in surface decreased from 92.1% to 86.7%, which indicated that HAC oxidation led to the formation of large amounts of oxygen-containing functional groups. Specifically, the proportion of various species on C-as received and C-HAC was very different. O 1s data indicated that –C═O groups increased from 55.2% to 58.8% and for C 1s XPS data, there was a little increase of –COO from 5.6% to 7.6%, but obvious increase was found for –C═O groups from 25.0% to 34.4% after HAC modification. Generally, the carbon functionalized by acetic acid significantly increased surface carbonyl groups. Some researchers reported that the increase of carboxylic groups on carbon surface enhanced the loading number of $PtCl^{6-}$, while carbonyl groups strengthened the adsorption of $PtCl^{6-}$ on carbon support [32,33]. In this work, it also exhibited that large amount of carbonyl groups presented on carbon surface after HAC treatment, which was in favor of stabilizing Pt nano-particle on carbon support. This was compatible with the less aggregation of Pt/C-HAC showed by Fig. 1e and f in Section 3.1.

For Pt/C-JM and Pt/C-HAC, the Pt 4f spectrum showed a little change. Depending on the oxidation state of Pt, there were two or three pairs of platinum peaks [29]. In Fig. 3e and f, the intensity of double shoulder peaks at 73.0 eV and 75.6 eV was quite low, which indicated very little PtO or $Pt(OH)_2$ [34] presented on both Pt/C-JM and Pt/C-HAC catalysts. The most intense ones, located around 71.2–71.8 eV and 74.3–74.7 eV, were due to metallic platinum Pt $4f_{7/2}$ and Pt $4f_{5/2}$. Due to the low ratio of Pt^{2+} in both samples, it is hard to obtain the value from the software, which exhibited that platinum mostly existed in the form of metal Pt^0. Additionally, the binding energy of metallic Pt on Pt/C-HAC shifted to the high value direction in Table 2, probably due to various electronic interactions between Pt and carbon support [35,36]. The phenomenon was a symbol of strong interaction between them, which also explained high anti-sintering ability of Pt/C-HAC than that of Pt/C-JM at high temperature.

3.4. The effect of HAC treatment on Pt/C electro-catalyst behavior

Cyclic voltammetry (CV) curves were obtained for Pt/C-JM and Pt/C-HAC in the potential range of −0.241 V to 1.2 V (vs. SCE) by a scan rate of 20 mV s^{-1}. The electrochemical active surface area of Pt/C catalysts can be estimated from hydrogen adsorption/desorption peaks of the cyclic voltammograms in Fig. 4a. Assuming a hydrogen monolayer adsorption charge of $Q^0 = 210\,\mu C\,cm^{-2}$ [37], the electrochemical active surface area (ESA) is calculated by $Q/[Pt]Q^0$, where Q is the charge transferred derived from the adsorption/desorption on the surface of platinum in −0.19 V to 0.16 V voltage range [38], and [Pt] represents the Pt loading in the electrode. According to Fig. 4a, the ESA increased from 71.3 for Pt/C-JM to 93.9 $m^2\,g^{-1}$ for Pt/C-HAC. That may be the result of the high dispersion and density of Pt nano-particles on functionalized carbon support.

The typical CV curves for methanol electro-oxidation on Pt/C catalysts are also shown in Fig. 4b. From the forward CV scans, the current peak of 7.54 mA for Pt/C-HAC was obtained at 0.882 V, which was much higher than 6.10 mA for Pt/C-JM at 0.948 V. The oxygen reduction reaction (ORR) of Pt/C-HAC activity was measured and illustrated in Fig. 4c. The Pt-HAC showed high onset potential of oxygen reduction and maximum current value. ORR activity with

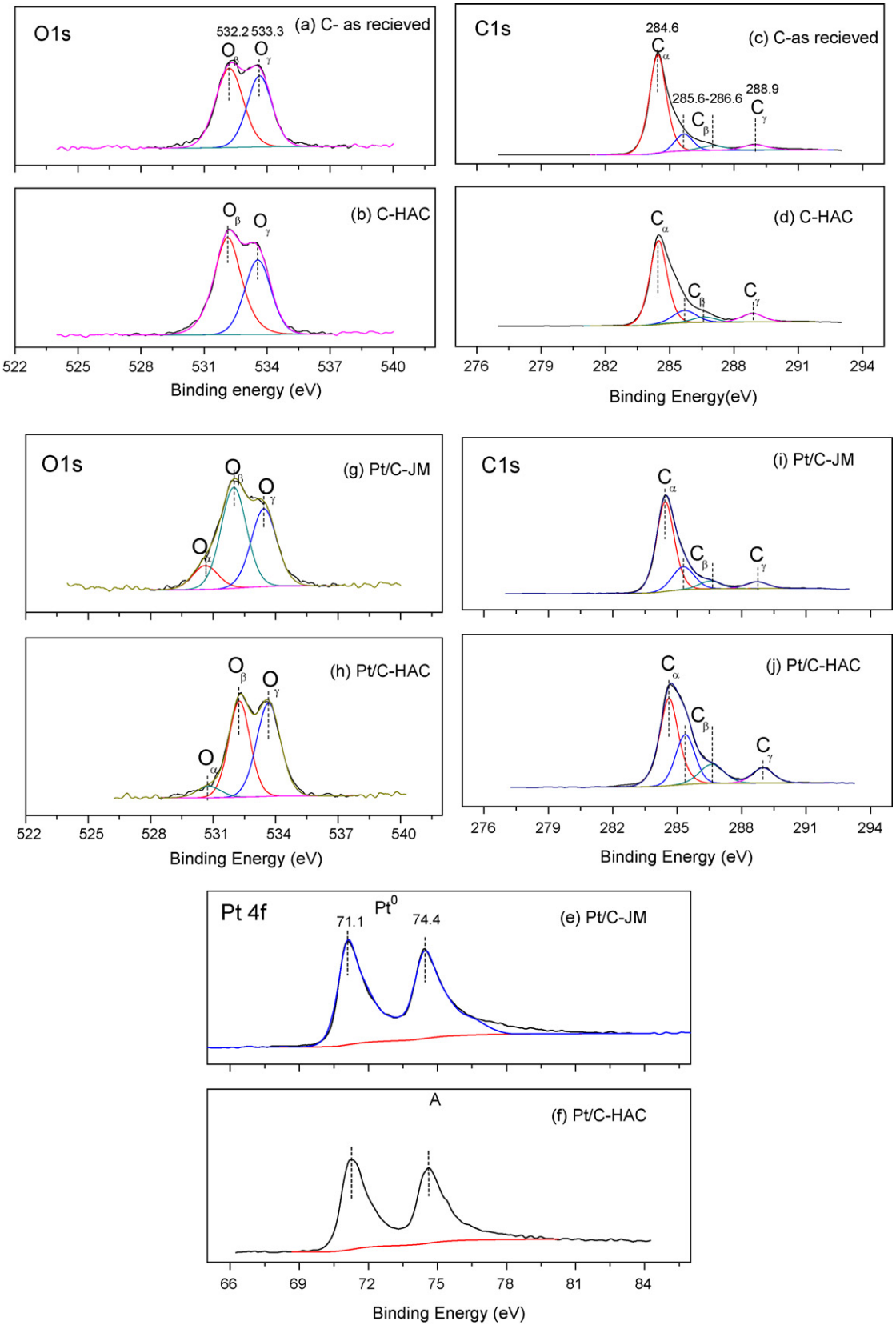

Fig. 3. C 1s O 1s and Pt 4f XPS spectra of C and Pt/C catalysts.

a reduction current of 0.785 mA for Pt/C-HAC was acquired, while only 0.385 mA for Pt/C-JM. These results implied that the catalytic activity for methanol oxidation and oxygen reduction improved obviously after HAC modification of carbon support.

The chronoamperometric data of Pt/C-HAC and Pt/C-JM with an aim of stability test was reported in Fig. 4d. The higher methanol oxidation current for Pt/C-HAC was able to maintain for over 2 h than that of Pt/C-JM catalyst. It was noted that Pt/C-HAC exhibited

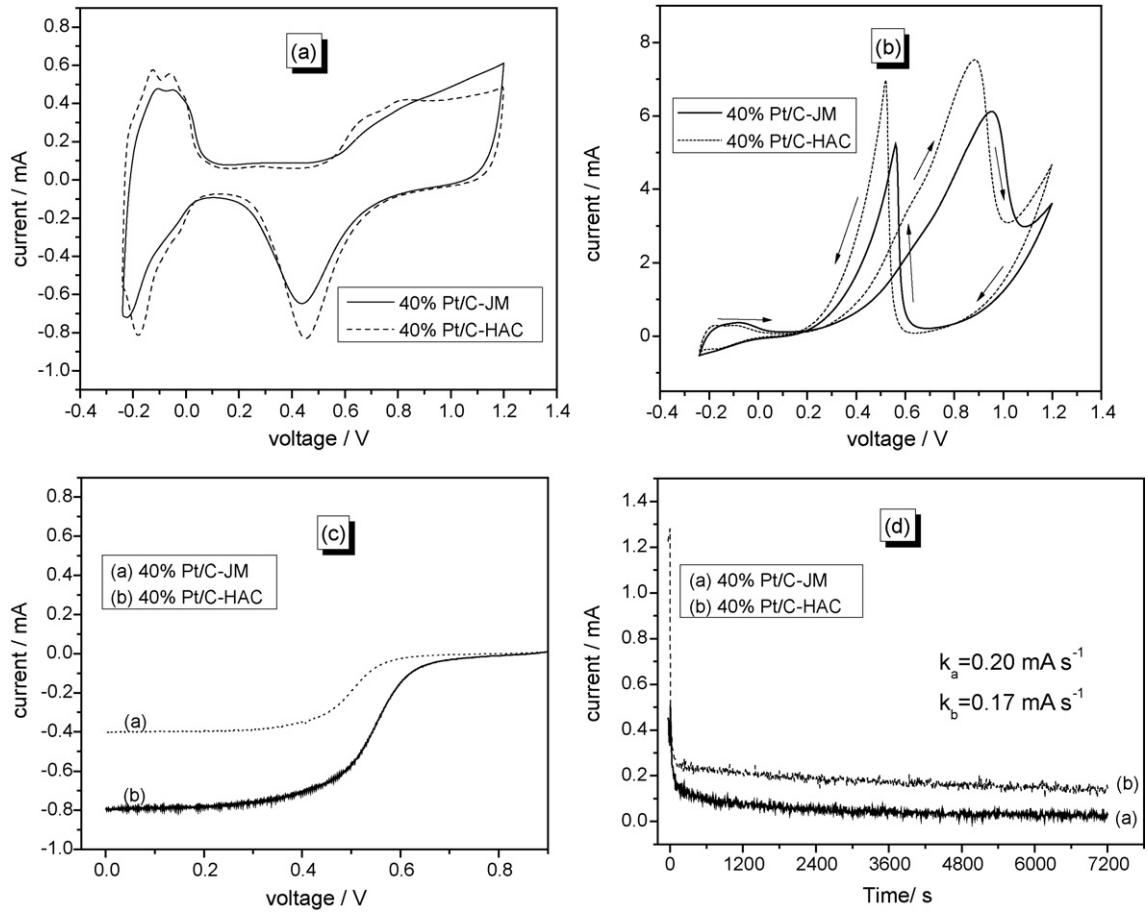

Fig. 4. (a) Cyclic voltammograms for Pt/C-JM and Pt/C-HAC. Scan rate = 20 mV s^{-1} at room temperature in 0.5 M H_2SO_4. (b) Cyclic voltammograms for Pt/C-JM and Pt/C-HAC. Scan rate = 20 mV s^{-1} at room temperature in 0.5 M H_2SO_4 + 0.5 M CH_3OH. (c) Polarization curves with a rotating disk electrode for the ORR on Pt/C-JM and Pt/C-HAC. Sweep rate: 5 mV s^{-1} at room temperature in O_2-saturated 0.5 M H_2SO_4, disk electrode area: 0.196 cm^2. (d) Chronoamperometric curves for methanol eletro-oxidation on Pt/C-JM and Pt/C-HAC catalysts in 0.5 M H_2SO_4 + 0.5 M CH_3OH.

slower decline rate of 0.17 mA s^{-1} than that of Pt/C-JM of 0.2 mA s^{-1}. The better electrochemical stability of Pt/C-HAC than Pt/C indicates that stronger interaction between Pt nano-particles and carbon support can be obtained after HAC treatment, which can also be confirmed by XRD and XPS results.

4. Conclusions

An alternative weak acid modified carbon was efficiently carried out to prepare highly dispersed Pt supported on carbon. BET, TEM and XPS analysis illuminated that acetic acid modified carbon had more microporous structure, narrower Pt particle-size distribution, sufficient carbonyl functional groups on surface compared with as-received carbon materials. Furthermore, TEM and XRD studies directly showed high Pt dispersion and density on HAC modified XC-72. The Pt/C-HAC catalyst presented a better methanol oxidation and oxygen reduction activity than that of Pt/C-JM catalyst. Moreover, XRD and TEM results present obvious signals to indicate that Pt/C-HAC is more stable than commercial Pt/C catalyst after high temperature heat treatment. The improvement of electrochemical performance and stability may be the result of high electrochemistry surface area and the formation of a large amount of carbonyl functional groups after HAC treatment. Therefore, the results indicate that HAC modification is one of effective ways to enforce the interaction between Pt and carbon support.

Acknowledgements

The authors gratefully acknowledge the financial support by National Basic Research Program of China (No. 2007CB613300), State Natural Sciences Foundation Monumental Projects (No. 50732004), Natural Science Foundation of Jiangsu Province (No. BK2008251) and Scientific Research Foundation for the Returned Overseas Chinese Scholars, State Education Ministry.

References

[1] H. Jankowska, A. Swiatkowski, J. Choma, Active Carbon, Ellis Horwood, New York, 1991.
[2] K.M. Guo, Z.L. Xie, L. Ma, C.Q. Yuan, New Carbon Mater. 2 (2001) 54–56.
[3] J.M. Solar, C.A. Leon, K. Osseo-Asare, L.R. Radovic, Carbon 28 (1990) 369–375.
[4] S.C. Roy, P.A. Christense, A. Hamnett, K.M. Thomas, V. Trapp, J. Electrochem. Soc. 143 (1996) 3073–3079.
[5] E. Auer, A. Freund, J. Pietsch, T. Tacke, Appl. Catal. A: Gen. 173 (1998) 259–271.
[6] M.C. Roman-Martinez, D. Cazorla-Amoros, A. Linares-Solano, C. Salinas-Martinez de Lecea, Carbon 31 (1993) 895–902.
[7] F. Coloma, A. Sepulveda-Escribano, J.L.G. Fierro, F. Rodriguez-Reinoso, Appl. Catal. A: Gen. 150 (1997) 165–183.
[8] L.R. Radovic, C. Sudhakar, in: H. Marsh, E.A. Heintz, F. Rod-riguez-Reinoso (Eds.), Introduction to Carbon Technologies, University of Alicante Publications, Alicante, 1997, pp. 103–166.
[9] J.L. Figueiredo, M.F.R. Pereira, M.M.A. Freitas, J.J.M. Orfao, Carbon 37 (1999) 1379–1389.
[10] J. Liu, A.G. Rinzler, H. Dai, J.H. Hafner, R.K. Bradley, P.J. Boul, A. Lu, T. Iverson, K. Shelimov, C.B. Huffman, F. Rodriguez-Macias, Y.S. Shon, T.R. Lee, D.T. Colbert, R.E. Smalley, Science 280 (1998) 1253–1256.
[11] T. Kyotani, S. Nakazaki, W.H. Xu, A. Tomita, Carbon 39 (2001) 782–785.

[12] D.B. Mawhinney, V. Naumenko, A.J. Kuznetsova, J.T. Yates, J. Liu, R.E. Smalley, J. Am. Chem. Soc. 122 (2000) 2383–2384.
[13] Z. Chen, R.H. Hauge, R.E. Smalley, J. Nanotechnol. 6 (2006) 1935–1938.
[14] R. Yu, L. Chen, Q. Liu, J. Lin, K.L. Tan, S.C. Ng, H.S.O. Chan, G.Q. Xu, A.T.S. Hor, Chem. Mater. 10 (1998) 718–722.
[15] Z. Li, W. Yan, S. Dai, Langmuir 21 (2005) 11999–12006.
[16] C. Prado-Burguete, A. Linares-Solano, F. Rodriguez-Reinoso, C. Salinas-Martibez, J. Catal. 115 (1989) 98–106.
[17] C. Prado-Burguete, A. Linares-Solano, F. Rodriguez-Reinoso, C. Salinas-Martibez, J. Catal. 128 (1991) 397–404.
[18] Q. Xie, X.L. Zhang, Q.R. Chen, G.Z. Gong, New Carbon Mater. 18 (2003) 203–208.
[19] Y. Xing, J. Phys. Chem. B 108 (2004) 19255–19259.
[20] J. Zhang, H. Zou, Q. Qing, Y. Yang, Q. Li, Z. Liu, X. Guo, Z. Du, J. Phys. Chem. B 107 (2003) 3712–3718.
[21] V. Lordi, N. Yao, J. Wei, Chem. Mater. 13 (2001) 733–737.
[22] C.K. Poh, S.H. Lim, H. Pan, J.Y. Lin, J.Y. Lee, J. Power Sources 176 (2008) 70–75.
[23] M.S. Wilson, F.H. Garzon, K.E. Sickafus, S. Gottesfeld, J. Electrochem. Soc. 140 (1993) 2872–2877.
[24] J. Xie, D.L. Wood III, K.L. More, P. Atanassov, R.L. Borup, J. Electrochem. Soc. 152 (2005) A1011–A1020.
[25] C. He, H.R. Kunz, J.M. Fenton, J. Electrochem. Soc. 144 (1997) 970–979.
[26] C. Grolleau, C. Coutanceau, F. Pierre, J.M. Leger, Electrochim. Acta 53 (2008) 7157–7165.
[27] W.M. Chen, Q. Xin, G.Q. Sun, Q. Wang, Q. Mao, H.D. Su, J. Power Sources 180 (2008) 199–204.
[28] J.L. Gomez de la Fuetnte, M.V. Martinez-Huerta, S. Rojas, P. Terreros, J.L.G. Fierro, M.A. Pena, Catal. Today 116 (2006) 422–432.
[29] V. Alderucci, L. Pino, P.L. Antonucci, W. Roh, J. Cho, H. Kim, D.L. Cocke, Mater. Chem. Phys. 41 (1995) 9–14.
[30] P. Albers, K. Deller, B.M. Despeyroux, A. Schafer, K. Seibold, J. Catal. 133 (1992) 467–478.
[31] J.B. Goodenough, A. Hamntt, B.J. Kennedy, R. Manoharan, S.A. Weeks, J. Electroanal. Chem. 240 (1988) 133–145.
[32] F. Rodriguez-Reinoso, Carbon 36 (1998) 159–175.
[33] X.W. Yu, S.Y. Ye, J. Power Sources 172 (2007) 133–144.
[34] D. Briggs, M.P. Seah, in: D. Briggs, M.P. Seah (Eds.), Practical Surface Analysis by Auger and X-ray Photoelectron Spectroscopy, Wiley, New York, 1990.
[35] A.K. Shukla, M.K. Ravikumar, A. Roy, S.R. Barman, D.D. Sarma, A.S. Arico, V. Antonucci, L. Pino, N. Giordano, J. Electrochem. Soc. 141 (1994) 1517–1522.
[36] A. Shukla, K. Ramesh, R. Manoharan, P. Sarode, S. Vasudevan, B. Bunsenges, Phys. Chem. 89 (1985) 1261–1267.
[37] B.L. Gratiet, H. Remita, G. Picq, M.O. Delcourt, J. Catal. 164 (1996) 36–43.
[38] S.H. Lim, J. Wei, J. Lin, Chem. Phys. Lett. 400 (2004) 578–582.